

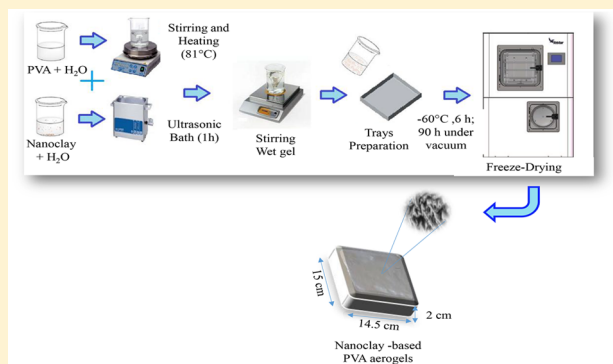
# Nanoclay-Based PVA Aerogels: Synthesis and Characterization

Carolina Simón-Herrero, Laura Gómez, Amaya Romero, José L. Valverde, and Luz Sánchez-Silva\*<sup>1</sup>

Department of Chemical Engineering, University of Castilla La Mancha, Av. Camilo José Cela 12, 13071 Ciudad Real, Spain

**S** Supporting Information

**ABSTRACT:** Nanoclay-based PVA aerogels have been synthesized at pilot-plant scale, using an environmentally friendly freeze-drying method. In the present work, the influence of different types of nanoclays on the physical, mechanical, and thermal properties of the resulted PVA aerogels were evaluated. In addition, the effect of nanoclay/PVA mass ratio was studied. Nanoclay incorporation into the polymeric matrix resulted in compact structures with small pore size distribution. Moreover, nanoclay addition (up to 3 wt %) allowed to improve the mechanical properties of the obtained aerogels. Nanoclay-based PVA aerogels showed interesting properties, such as high lightness, good mechanical properties, low thermal conductivity, and fire resistance.



## 1. INTRODUCTION

Organic aerogels are ultralight materials with a framework mainly based on organic polymers. Furthermore, they have better mechanical properties than inorganic aerogels.<sup>1</sup> However, polymers are known for their relatively high flammability, because of the chemical composition, which consists mainly of carbon and hydrogen. Furthermore, most of them are accompanied by toxic gases during the combustion.<sup>2</sup> Thus, it is interesting to improve the flame-retardant properties associated with the polymeric aerogels in order to expand the application field of these interesting materials.<sup>3</sup>

Flame-retardant additives are an essential part of polymer formulations to reduce risks in fire situations. Although a large variety of conventional flame retardants such as brominated organic compounds<sup>4</sup> and inorganic fillers<sup>5</sup> are known, new materials, which improve the thermal, mechanical, and flame-retardant properties, such as nanomaterials, are being investigated. In this regard, nanoclays are considered to be a good alternative to improve the flame-retardant properties of polymeric aerogels.<sup>2,6,7</sup>

Clay-based aerogels are ultralight materials that present a “house of cards”-like structure,<sup>8</sup> using a clay suspension by means of an environmentally friendly freeze-drying process.<sup>9</sup> In this method, the material to be dried is frozen and then, under a high vacuum, is heated (by conduction or radiation or by both) so that frozen liquid sublimates,<sup>10</sup> allowing the production of high-quality clay aerogels with enhanced properties, such as high Young’s modulus, low gas permeability, and fire-resistant properties.<sup>8</sup> Clay-based aerogels present a lamellar structure with a layer thickness in the range of 1–4  $\mu\text{m}$  and interlayer distances of 20–100  $\mu\text{m}$ .<sup>8</sup> Furthermore, because of the abundance of clay in nature, its easy processing and its resistance to ignition make the clay-based aerogel a very competitive material.<sup>11,12</sup>

Poly(vinyl alcohol) (PVA) is a water-soluble polymer produced by the hydrolysis of polyvinyl acetate. PVA is biodegradable and can provide good properties as toughness and flexibility at relatively low cost.<sup>13</sup> Clay aerogels and polymer aerogels present poor mechanical properties. One way to improve these properties is to combine a water-soluble polymer solution into a clay dispersion. Furthermore, PVA is a good candidate for the production of clay aerogels, because of the strong attraction between the hydrogen present in the polymer and the oxygen in the lattice of the clay.<sup>8,14,15</sup>

PVA allows one to obtain interesting clay-based aerogels as a consequence of their low-cost production, their good mechanical properties, and their nontoxicity.

The aim of the present work was to develop nanoclay-based PVA aerogels using a freeze-drying process at pilot-plant scale to dry the wet gel. Furthermore, carbon nanofibers reinforced polymer aerogels and PVA aerogels were also synthesized to compare their properties with those of the nanoclay-based polymer aerogels. Moreover, the influence of the nanoclay (nanoclay/PVA) mass ratio on the morphological, mechanical, and thermal properties was evaluated in detail, as well as its impact on the flame-retardant properties of the resulting materials.

## 2. EXPERIMENTAL SECTION

**2.1. Materials.** Poly(vinyl alcohol) (10–98, Mw 61 000 g/mol) of analytical grade was supplied by Fluka Chemical Co. Hydrophilic bentonite nanoclay and montmorillonite nanoclay with surface modification (35–45 wt % dimethyl dialkyl amine)

Received: January 24, 2018

Revised: March 29, 2018

Accepted: April 13, 2018

Published: April 13, 2018

Table 1. Denomination and Characterization of Obtained Nanoclay-Based PVA Aerogels

sample <sup>a</sup>	nanoclay type <sup>b</sup>	nanoclay/PVA (wt %)	density (g/cm <sup>3</sup> )	Young's modulus (MPa)	T <sub>g</sub> (°C)	k (W/(m K))
HNPA0.25	H	0.25	0.046	0.26	76.4	0.029 ± 0.001
HNPA1	H	1	0.052	0.56	77.4	0.032 ± 0.001
HNPA3	H	3	0.065	1.56	80.7	0.039 ± 0.001
HNPA5	H	5	0.081	0.34	77.1	0.044 ± 0.001
HNPA10	H	10	0.107	0.28	78.1	0.051 ± 0.002
SNPA0.25	S	0.25	0.043	0.32	78.3	0.030 ± 0.001
SNPA1	S	1	0.054	0.86	81.2	0.035 ± 0.001
SNPA3	S	3	0.078	4.90	80.1	0.041 ± 0.001
SNPA5	S	5	0.090	1.02	76.6	0.050 ± 0.002
SNPA10	S	10	0.118	0.31	78.1	0.052 ± 0.002

<sup>a</sup>HNPA<sub>i</sub> = hydrophilic nanoclay-based PVA aerogel with *i* wt % of hydrophilic nanoclay related to the amount of PVA. SNPA<sub>i</sub> = surface-modified nanoclay-based PVA aerogel with *i* wt % of surface nanoclay, related to the amount of PVA. <sup>b</sup>H = hydrophilic bentonite nanoclay. S = nanoclay with surface modification (35–45 wt % dimethyl dialkyl amine).

were supplied by Sigma–Aldrich Co., Ltd. Carbon nanofibers (CNFs), which are used as reinforcing material, were obtained according to the procedure described by Jimenez et al.<sup>16</sup> Water was purified by distillation, followed by deionization using ion-exchange resins.

**2.2. Preparation of Nanoclay-Based PVA Aerogels at Pilot-Plant Scale.** Nanoclay-based PVA aerogels were prepared at pilot-plant scale (freeze-drying unit with a production of 2 m<sup>2</sup> of aerogel per batch) by following a procedure based on that reported in previous works.<sup>1,10,17</sup> Table 1 lists the studied samples.

A solution of poly(vinyl alcohol) in deionized water (2.5 wt %) was prepared by heating at 81 °C under vigorous stirring until its complete dissolution. The corresponding amount of nanoclay (from 0.25 to 10 wt %, relative to the total amount of polymer) was dispersed in water using an ultrasonic bath (1 h at room temperature). Then, both solutions (at room temperature) were mixed under vigorous stirring to obtain the wet gel (600 mL), which was then deposited into the freeze-drying trays with dimensions of 14.5 cm (long) × 15 cm (high) × 2 cm (wide), frozen for 6 h at –60 °C and, finally, sublimated under vacuum for 90 h. Finally, aerogels with the same dimensions of the trays of the freeze-drying were obtained.

Carbon-nanofiber-reinforced polymer aerogels and PVA aerogels were synthesized as reported in previous works<sup>1,10</sup> (see Table 2).

Table 2. Denomination and Characterization of Carbon Nanofibers Reinforced Polymer Aerogels and PVA Aerogels

sample <sup>a</sup>	PVA (wt %)	carbon nanofibers, CNFs (wt %)	Young's modulus (MPa)	T <sub>g</sub> (°C)	k (W/(m K))
PVAA	100	0	0.23	77.7	0.028 ± 0.001
CNFs0.25	99.75	0.25	0.77	76.1	0.049 ± 0.001

<sup>a</sup>PVAA = PVA aerogels. CNFs0.25 = PVA aerogels reinforced with 0.25 wt % CNFs.

**2.3. Characterization of Nanoclay-Based PVA Aerogels.** The morphological structure was analyzed using a scanning electron microscopy (SEM) system (Model Phenom-ProX, Phenom World) that was equipped with an energy-dispersive X-ray spectroscopy (EDS) probe to determine the average composition of the aerogels. To analyze the pore size distribution and the density of the aerogels in detail, a mercury

porosimeter (Quantachrome Poremaster) was used. The methodology is based on the physical penetration of mercury into the pores of the materials when a sufficient pressure is applied to allow it to intrude. The resulting mercury volume registration, as a function of increasing pressure, allows the generation of the pore size distribution.<sup>18</sup>

The Young's modulus was determined using dynamic mechanical analysis (DMA) 1 STARE System (Mettler Toledo), through the application of stress–strain analysis in compression mode.

Differential scanning calorimetry (DSC) was performed in a DSC 2 STARE System supplied by Mettler Toledo to determine the glass-transition temperature (T<sub>g</sub>). Measurements were performed by varying the temperature between 20 °C and 200 °C with a heating (or cooling) rate of 10 °C/min in a nitrogen atmosphere.

Thermal conductivity measurements were performed by using a Heat Flow Meter (LINSEIS HFM 300) with a high level of accuracy. The instrument is designed per ASTM C518, JIS A1412, ISO 8301, and DIN 12667. The methodology is based on the heat flow measurements when a sample is located between a hot plate and a cold plate. It allows one to determine thermal conductivities in a wide range from 0.001 W/(m K) to 2.5 W/(m K). Furthermore, it can operate at different temperatures (from –30 °C to 90 °C). Thermogravimetric analysis (TGA) (using a thermal analyzer (Mettler Toledo TGA/DSC 1 STARE System) was carried out to study the behavior of the synthesized aerogels with the temperature. Combustion was carried out at a heating rate of 10 °C/min under an air atmosphere using a gas flow of 100 N mL/min. In order to investigate the flame-retardant properties of the materials, nanoclay-based PVA aerogels were also ignited.

### 3. RESULTS

In previous works, the synthesis of carbonaceous nanomaterial-reinforced polymer aerogels using freeze-drying to dry the wet gel was performed and, the influence of the polymer nature on the aerogels characteristics was evaluated.<sup>1,10</sup> Characterization results using both scanning electron microscopy (SEM) and nitrogen adsorption–desorption isotherms showed that poly(vinyl alcohol) (PVA) was the most suitable polymer to obtain aerogels with very light density and high surface area.<sup>17</sup> In addition, the use of different solvents and the influence of the mass ratio of PVA/CNFs in the synthesis of CNF-reinforced polymer aerogels were also studied. Thus, 0.25 wt % CNFs was selected as the best carbon nanomaterial amount, because of

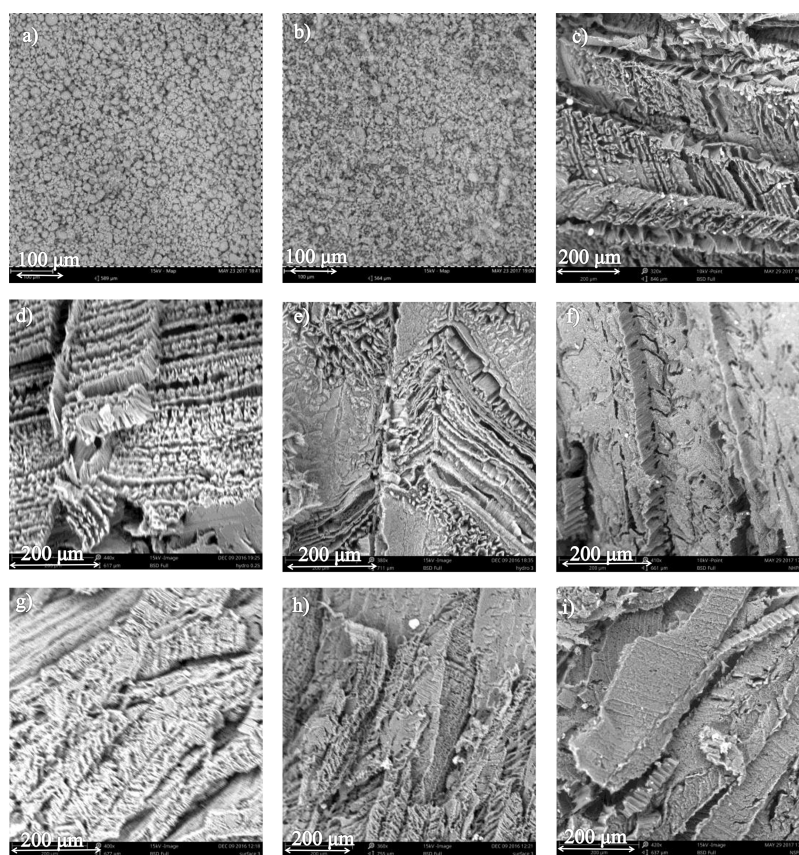


**Figure 1.** SEM micrograph of samples: (a) hydrophilic nanoclay (HN), (b) nanoclay with surface modification (SN), (c) PVA aerogel (PVAA), (d) HNPA0.25, (e) HNPA3, (f) NPA10, (g) SNPA0.25, (h) SNPA3, and (i) SNPA10.

the final product showed the lowest thermal conductivity and appropriate mechanical properties.<sup>1</sup> In this study, nanoclay-based PVA aerogels with several percentages of different nanoclays (hydrophilic nanoclay and nanoclay with surface modification) were synthesized and then characterized. Their properties were compared to those of the carbon-nanofiber-reinforced polymer aerogels and PVA aerogels reported in the above-mentioned prior study.<sup>1</sup>

**3.1. Study of the Physicochemical and Morphological Properties of Nanoclay-Based PVA Aerogels.** SEM analysis was carried out in order to study the effect of the nanoclay addition on the morphological properties of the resulting aerogels. Figure 1 shows SEM micrographs of the nanoclays (hydrophilic and nanoclay with surface modification; see Figures 1a and 1b, respectively), PVA aerogels (Figure 1c), hydrophilic nanoclay-based PVA aerogels (HNPA, Figures 1d, 1e, and 1f) and surface-modified nanoclay-based PVA aerogels (SNPA, Figures 1g, 1h, and 1i).

As can be clearly observed, nanoclay incorporation into the polymeric matrix resulted in a remarkable impact on the morphology of the aerogels. Thus, the formation of lamellar porous structures, typical of PVA aerogel, were observed when the nanoclay/PVA mass ratio was low (up to 3 wt %). Furthermore, the addition of nanoclay resulted in a change on the structure; hence, the network appeared denser, which was attributed to aggregation of the nanoparticles.<sup>19</sup> These findings were in good agreement with the results obtained from mercury porosimetry analysis.

Figure 2 shows the pore size distribution of the different nanoclay-based PVA aerogels. It can be seen that the amount of

nanoclay also had an effect on the porosity of the resulting aerogels. The higher the nanoclay/PVA mass ratio was, the smaller the pore diameters were. The peak height (intruded volume into the pores of the sample) of the pore size distribution (PSD) decreased with the addition of nanoclay, since its incorporation into the polymeric matrix resulted in compact structures, as a consequence of the particle agglomeration. Thus, the apparent density of the nanoclay-based PVA aerogels increased with nanoclay addition (Table 1).

EDS microanalysis was carried out to corroborate the presence of nanoclays into the polymeric matrix. Oxygen and silicon were mainly detected in the hydrophilic nanoclay by the EDS analysis. Furthermore, aluminum was also detected. Regarding the nanoclay with surface modification, the EDS analysis showed characteristic groups of montmorillonite clay (oxygen, silicon, aluminum, magnesium, and sodium) and carbon, and nitrogen associated with the dimethyl dialkyl amine present in the nanoclay. EDS analysis of nanoclay-based PVA aerogels showed the characteristics groups of nanoclays and carbon, as a consequence of the presence of PVA and, in the corresponding samples, nanoclay with surface modification.

**3.2. Study of the Mechanical Properties of Nanoclay-Based PVA Aerogels.** Mechanical properties of the aerogels were determined by using DMA equipment. A stress–strain analysis was performed to determine the Young's modulus.

Figures 3 and 4 show the stress–strain curves for the aerogels obtained using different nanoclay/PVA mass ratios. Each curve represents the experienced strain when small stresses are applied. The elastic modulus (or Young's modulus) was

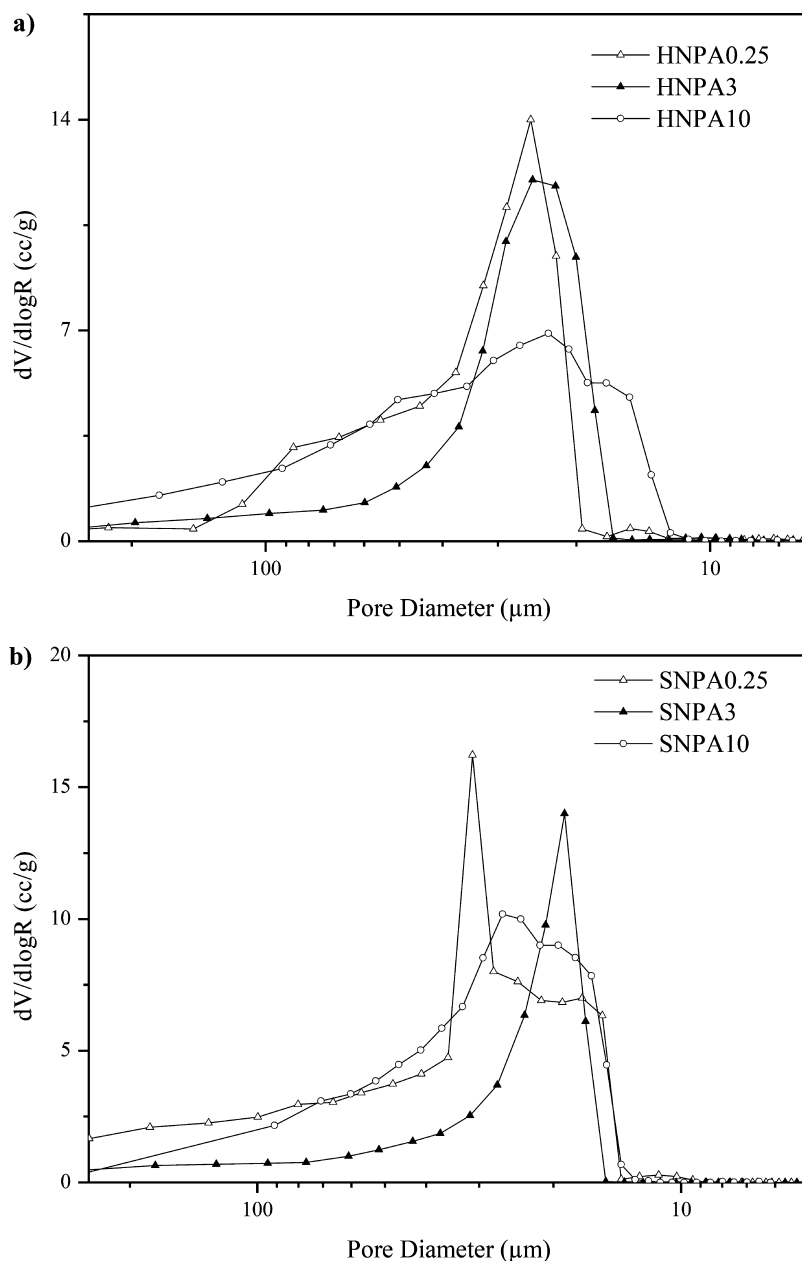


**Figure 2.** Pore size distribution of (a) hydrophilic nanoclay-based PVA aerogels and (b) surface-modified nanoclay-based PVA aerogels.

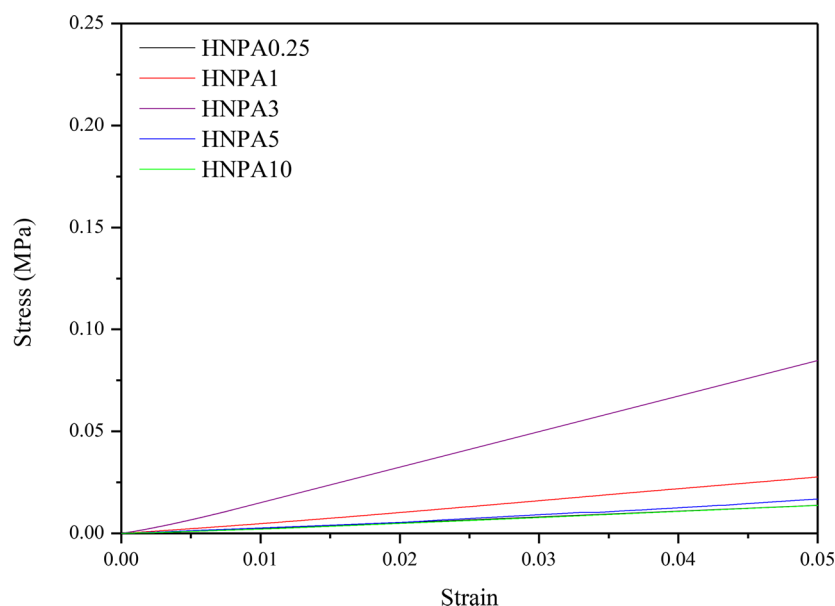
determined from the slope of the linear part of the stress–strain curve, where an elastic behavior of the aerogels was observed (Table 1). It has been considered to have a strain range from 0 to 0.05, because it was the region with an elastic behavior.

Figure 3 and 4 show that the incorporation of nanoclays into the polymeric matrix improved the mechanical properties of the nanoclay-based PVA aerogels up to a nanoclay percentage of 3 wt%. Thus, aerogel synthesized using 3 wt% nanoclays presented the smallest strain and the highest Young's modulus (Table 1). In other words, the high viscosity of those samples synthesized with high percentages of nanoclays did not favor the mechanical properties of the resulting materials. Furthermore, the higher the nanoclay concentration, the smaller the contact surface area, which resulted in a weak adhesion between the polymeric matrix and the nanoclay. As consequence, the tensile strength decreased. Moreover, as previously mentioned, the agglomeration of nanoparticles could

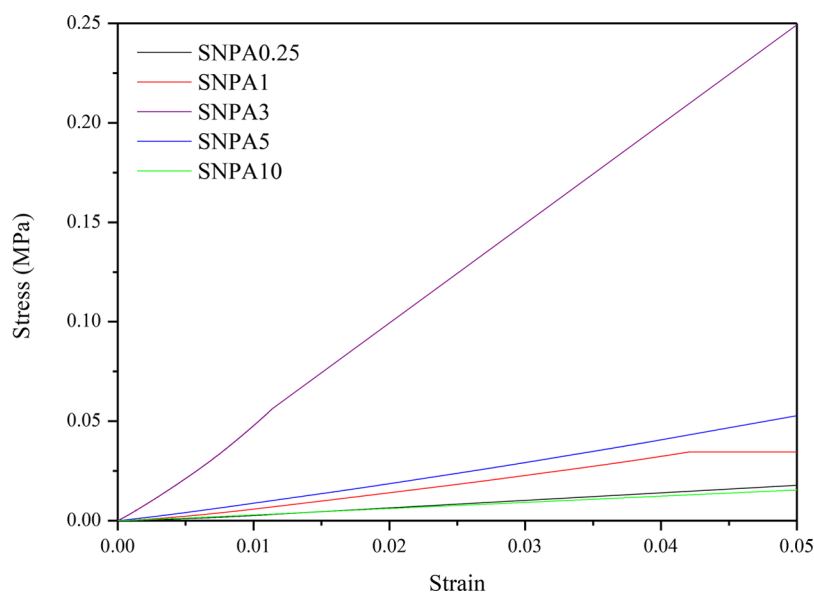
also negatively affect the mechanical performance of these materials.<sup>20</sup>

Figure 5 shows the stress–strain analysis of samples PVAA, CNFs0.25, HNPAs0.25, and SNPAs0.25. As observed, sample CNFs0.25 presented a higher value of Young's modulus (see Tables 1 and 2) than those aerogels synthesized with the same nanoclay concentration (for both types of nanoclays). Small amounts of carbonaceous nanomaterials resulted in an improvement of the mechanical properties of the resulting aerogels as demonstrated elsewhere.<sup>1</sup> Thus, it could be concluded that the presence of CNFs in the aerogel improved the mechanical performance in a higher extension than that of nanoclays.

**3.3. Study of the Thermal Properties of Nanoclay-Based PVA Aerogels.** A thermal conductivity analysis was also evaluated to determine the thermal properties of the different aerogels. Thermal conductivity can be affected by



**Figure 3.** Stress–strain analysis of hydrophilic nanoclay-based PVA aerogels (HNPA) with different percentages of nanoclays (HNPA0.25, HNPA1, HNPA3, HNPA5, and HNPA10).



**Figure 4.** Stress–strain analysis of surface-modified nanoclay-based PVA aerogels (SNPA) with different percentages of nanoclays (SNPA0.25, SNPA1, SNPA3, SNPA5, and SNPA10).

several factors such as temperature, density, porosity, moisture, and sample surface.<sup>21</sup> It was observed, after performing repeated measurements for all samples, that the values of the thermal conductivity increased with nanoclay addition, as a consequence of the increase in density and the decrease in porosity. The increase in solids content leads to higher thermal conductivities. However, the porosity increase results in a better heat insulation property.<sup>3,21</sup> As seen, all the aerogels tested have very low thermal conductivities, lower than 0.055 W/(m K).

Furthermore, the glass-transition temperature ( $T_g$ ) (Table 1) of the synthesized aerogels were slightly higher (ranging from 76.5 °C to 81.3 °C) than that of the parent PVA (74.2 °C). This behavior is generally due to increases in  $T_g$  with the incorporation of high-temperature stable nanoscale reinforcement into the polymeric matrix. In some cases, there is an

absence of  $T_g$  improvement as a consequence of the incomplete dispersion of the nanoclay.<sup>22</sup>

Thermal stability of samples, which has been related to the weight loss percentage, as a function of temperature in an oxygen atmosphere, was determined using a thermogravimetric analyzer (TGA) (represented in Figure S1 in the Supporting Information). Figure S1a shows the weight loss curves of the parent PVA, the hydrophilic nanoclay (HN), and the hydrophilic nanoclay-based PVA aerogels (with the lowest and the highest concentration of nanoclay). The parent PVA presented three decomposition stages. The first one, which occurred in the range of 25–100 °C, was associated with the elimination of water (~2.5 wt %). The second decomposition stage, which ranged from 230 °C to 500 °C, represented the main weight loss in the combustion process and was due to the PVA decomposition. As shown, the nanoclay/PVA mass ratio

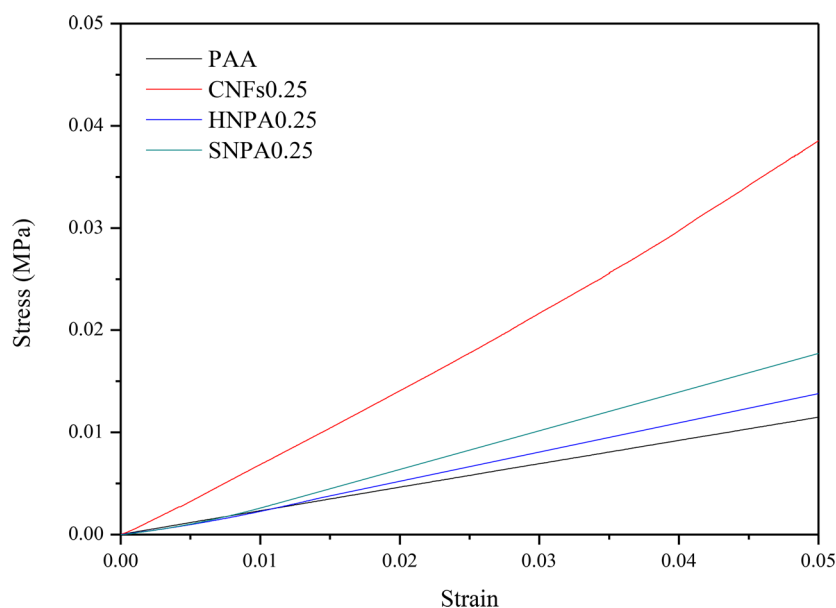


Figure 5. Stress–strain of samples HNPA0.25, SNPA0.25, PAA, and CNFs0.25.

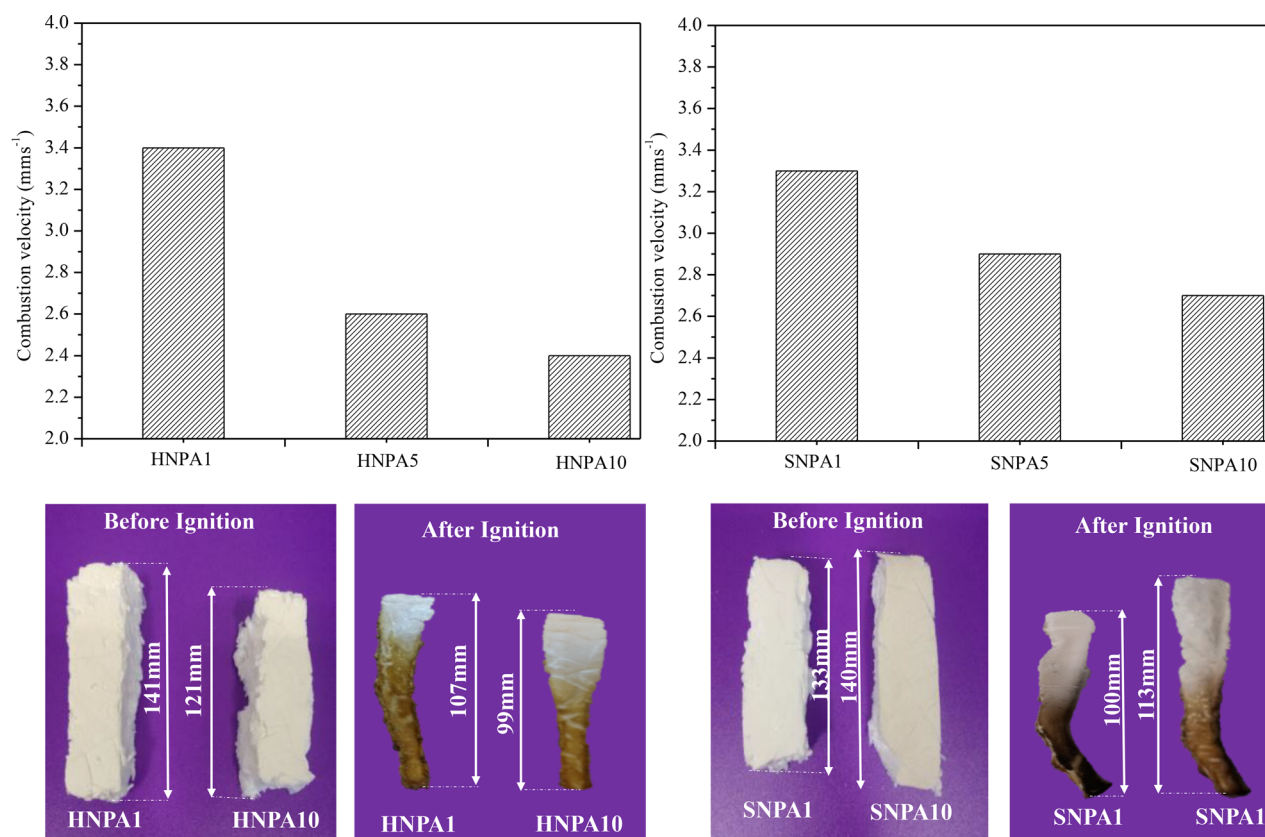


Figure 6. Combustion velocity, as a function of nanoclay content.

had an effect on the thermal behavior of the synthesized aerogels. The TGA curve of sample HNPA0.25 overlapped with that obtained for the parent PVA, because of the small amount of nanoclay present in the polymeric matrix. However, sample HNPA10 exhibited the highest thermal stability of all synthesized hydrophilic nanoclay-based PVA aerogels, which could be attributed to the interaction of the nanoclay with the polymeric matrix. At temperatures above 375 °C, curves shifted to higher temperatures as the amount of nanoclay increases.

Finally, the weight loss became almost constant above 550 °C. Sample HNPA0.25 presented residues of 10 wt %, whereas, for sample HNPA10, residue amounts reached up to 20 wt %, which was directly linked with the percentage of nanoclay existing within it.

Figure S1b shows the weight loss curves of the parent PVA, the montmorillonite nanoclay with surface modification (SN), and the surface-modified nanoclay-based PVA aerogels (with the lowest and the highest concentrations of nanoclay). TGA

curves were similar as those obtained for hydrophilic nanoclay-based PVA aerogels. As previously mentioned for hydrophilic nanoclay-based PVA aerogels, the TGA curve of sample SNPA0.25 overlapped with that obtained for the parent PVA, because of the small amount of nanoclay present in the polymeric matrix. However, sample SNPA10 exhibited the highest thermal stability of all synthesized surface-modified nanoclay-based PVA aerogels. The second decomposition stage, which represented the main weight loss of sample SNPA10, was due to the PVA and amine groups degradation.

In order to analyze the flame retardancy performance of the nanoclay-based PVA aerogels prepared here, samples were ignited and the combustion velocity was calculated after 10 s of ignition (see Figure 6). The combustion velocity decreased from 3.4 mm s<sup>-1</sup> to 2.4 mm s<sup>-1</sup> and from 3.3 mm s<sup>-1</sup> to 2.7 mm s<sup>-1</sup> with increasing nanoclay/PVA mass ratio for hydrophilic nanoclay-based PVA aerogels and surface-modified nanoclay-based PVA aerogels, respectively. These results would clearly indicate that the nanoclay incorporation into the polymeric matrix could increase the flame retardancy of the resulting nanoclay-based polymer aerogels. The burning process of polymeric materials begins with heating to a temperature at which thermal degradation initiates. The degradation products are superheated and nucleated to form bubbles. One flame-retardant approach is to suppress the bubbling rate.<sup>23</sup> Nanoclay particles reduced the flammability of polymeric materials by inhibiting the vigorous bubbling process in the course of the degradation process during combustion.<sup>7</sup> Montmorillonite clay has a high aspect ratio in a well-dispersed nanocomposite with a high surface area of 750 m<sup>2</sup> g<sup>-1</sup>, as reported by Kim et al.,<sup>24–26</sup> showing a good flame-retardancy when it is added to a polymeric matrix as a nanofiller.<sup>26</sup>

Summarizing, the synthesized nanoclay-based PVA aerogels present good mechanical and morphological properties, as well as appropriate thermal stability. Besides, nanoclay-based PVA aerogels are nontoxic materials with flame-retardant properties.

#### 4. CONCLUSIONS

Nanoclay-based PVA aerogels have been successfully synthesized at pilot-plant scale using an environmentally friendly and low-cost freeze-drying process. The nanoclay incorporation into the polymeric matrix resulted in a lower porosity and compact structures with small pore size due to the agglomeration of the particles. Furthermore, the nanoclay addition into the polymeric matrix allowed one to improve the mechanical properties of the aerogels. It was demonstrated that the nanoclay incorporation into the polymeric matrix improved the thermal stability of the aerogels. The synthesized materials have good heat insulation performance and exhibited appropriate flame-retardant properties.

#### ■ ASSOCIATED CONTENT

##### 📄 Supporting Information

The Supporting Information is available free of charge on the ACS Publications website at DOI: 10.1021/acs.iecr.8b00385.

TGA curves of parent PVA, HN, HNPA0.25, HNPA10, SN, SNPA0.25, and SNPA10 samples (PDF)

#### ■ AUTHOR INFORMATION

##### Corresponding Author

\*E-mail: [Marialuz.sanchez@uclm.es](mailto:Marialuz.sanchez@uclm.es).

#### ORCID

Luz Sánchez-Silva: 0000-0002-4348-7520

#### Notes

The authors declare no competing financial interest.

#### ■ ACKNOWLEDGMENTS

The present work was performed within the framework of the NANOLEAP project. This project has received funding from the European Union's Horizon 2020 Research and Innovation Program, under Grant Agreement No. 646397.

#### ■ REFERENCES

- (1) Víctor-Román, S.; Simón-Herrero, C.; Romero, A.; Gracia, I.; Valverde, J. L.; Sánchez-Silva, L. CNF-reinforced polymer aerogels: influence of the synthesis variables and economic evaluation. *Chem. Eng. J.* **2015**, *262*, 691–701.
- (2) Laoutid, F.; Bonnaud, L.; Alexandre, M.; Lopez-Cuesta, J. M.; Dubois, Ph. New prospects in flame retardant polymer materials: From fundamentals to nanocomposites. *Mater. Sci. Eng., R* **2009**, *63*, 100–125.
- (3) Han, Y.; Zhang, X.; Wu, X.; Lu, C. Flame retardant, heat insulating cellulose aerogels from waste cotton fabrics by in situ formation of magnesium hydroxide nanoparticles in cellulose gel nanostructures. *ACS Sustainable Chem. Eng.* **2015**, *3*, 1853–1859.
- (4) de Wit, C. A. An overview of brominated flame retardants in the environment. *Chemosphere* **2002**, *46* (5), 583–624.
- (5) Morgan, A. B.; Putthanarat, S. Use of inorganic materials to enhance thermal stability and flammability behaviour of a polyimide. *Polym. Degrad. Stab.* **2011**, *96* (1), 23–32.
- (6) Knight, C. C.; Ip, F.; Zeng, C.; Zhang, C.; Wang, B. A highly efficient fire-retardant nanomaterial based on carbon nanotubes and magnesium hydroxide. *Fire Mater.* **2013**, *37*, 91–99.
- (7) Shan, G.; Jin, W.; Chen, H.; Zhao, M.; Surampalli, R.; D, W.R.E. P.E.; Ramakrishnan, A.; Zhang, T.; P, E.; Tyagi, R. D. Flame retardant polymer nanocomposites and their heat-release rates. *J. Hazard., Toxic Radioact. Waste* **2015**, *19* (4), 04015006.
- (8) Madyan, O. A.; Fan, M.; Feo, L.; Hui, D. Enhancing mechanical properties of clay aerogel composites: An overview. *Composites, Part B* **2016**, *98*, 314–329.
- (9) Wang, Y.; Gawryla, M. D.; Schiraldi, D. A. Effects of freezing conditions on the morphology and mechanical properties of clay and polymer/clay aerogels. *J. Appl. Polym. Sci.* **2013**, *129* (3), 1637–1641.
- (10) Simón-Herrero, C.; Caminero-Huertas, S.; Romero, A.; Valverde, J. L.; Sánchez-Silva, L. Effects of freeze-drying conditions on aerogels properties. *J. Mater. Sci.* **2016**, *51*, 8977–8985.
- (11) Huang, P.; Fan, M. Development of fracture free clay-based aerogel: Formulation and architectural mechanisms. *Composites, Part B* **2016**, *91*, 169–175.
- (12) Gilman, J. W. Flammability and thermal stability studies of polymer layered-silicate (clay) nanocomposites. *Appl. Clay Sci.* **1999**, *15*, 31–49.
- (13) Jang, J.; Lee, D. K. Plasticizer effect on the melting and crystallization behavior of polyvinyl alcohol. *Polymer* **2003**, *44* (26), 8139–8146.
- (14) Karimi, A.; Wan Daud, W. M. A. Materials, preparation, and characterization of PVA/MMT nanocomposite hydrogels: A review. *Polym. Compos.* **2017**, *38*, 1086–1102.
- (15) Podsiadlo, P.; Kaushik, A. K.; Arruda, E. M.; Waas, A. M.; Shim, B. S.; Xu, J.; Nandivada, H.; Pumplun, B. G.; Lahann, J.; Ramamoorthy, A.; Kotov, N. A. Ultrastrong and stiff layered polymer nanocomposites. *Science* **2007**, *318* (5847), 80–83.
- (16) Jimenez, V.; Nieto-Marquez, A.; Diaz, J. A.; Romero, R.; Sanchez, P.; Valverde, J. L.; Romero, A. Pilot Plant Scale Study of the Influence of the Operating Conditions in the Production of Carbon Nanofibers. *Ind. Eng. Chem. Res.* **2009**, *48*, 8407–8417.

(17) Sánchez-Silva, L.; Víctor-Román, S.; Romero, A.; Gracia, I.; Valverde, J. L. Tailor-made aerogels based on carbon nanofibers by freeze-drying. *Sci. Adv. Mater.* **2014**, *6*, 665–673.

(18) Simón-Herrero, C.; Romero, A.; Valverde, J. L.; Sánchez-Silva, L. Hydroxyethyl cellulose/alumina-based aerogels as lightweight insulating materials with high mechanical strength. *J. Mater. Sci.* **2018**, *53* (1), 1556–1567.

(19) Ghaffari, T.; Barzegar, A.; Hamed; Rad, F.; Moslehifard, E. Effect of Nanoclay on Thermal Conductivity and Flexural Strength of Polymethyl Methacrylate Acrylic Resin. *J. Dent. Shiraz. Univ. Med. Sci.* **2016**, *17* (2), 121–127.

(20) Chowdary, M. S.; Kumar, M. S. R. N. Effect of Nanoclay on the Mechanical properties of Polyester and S-Glass Fiber (Al). *Int. J. Adv. Sci. Technol.* **2015**, *74*, 35–42.

(21) Shen, P.; Zhao, H.-B.; Huang, W.; Chen, H.-B. Poly(vinyl alcohol)/clay aerogel composites with enhanced flame retardancy. *RSC Adv.* **2016**, *6*, 109809–109814.

(22) Gupta, N.; Pinisetty, D.; Shunmugasamy, V. C. *Reinforced Polymer Matrix Syntactic Foams: Effect of Nano and Micro-Scale Reinforcement*; Springer Science & Business Media: Cham, Switzerland, 2013.

(23) Kashiwagi, T.; Mu, M.; Winey, K.; Cipriano, B.; Raghavan, S. R.; Pack, S.; Rafailovich, M.; Yang, Y.; Grulke, E.; Shields, J.; Harris, R.; Douglas, J. Relation between the viscoelastic and flammability properties of polymer Nanocomposites. *Polymer* **2008**, *49*, 4358–4368.

(24) Kahr, G.; Madsen, F. T. Determination of the cation exchange capacity and the surface area of bentonite, Illite and kaolinite by methylene blue adsorption. *Appl. Clay Sci.* **1995**, *9*, 327–336.

(25) Manias, E.; Touny, A.; Wu, L.; Strawhecker, K.; Lu, B.; Chung, T. C. Polypropylene/montmorillonite nanocomposites. Review of the synthetic routes and materials properties. *Chem. Mater.* **2001**, *13*, 3516–3524.

(26) Kim, H.; Park, J. J. W.; Kim, H. J. Flame retardant nanocomposites containing nanofillers. In *Tailored Nanostructures*; Di Sia, P., Ed.; One Central Press: 2016; Chapter 1, pp 1–28.